Polymer Physics and Structure/Property Relationships of Thermally Stable Polyarylene Ethers for Second-Order Nonlinear Optics

C. Y. Stacey Fu† and Hilary S. Lackritz*

School of Chemical Engineering, Purdue University, West Lafayette, Indiana 47907-1283

Duane B. Priddy, Jr.‡ and James E. McGrath

Department of Chemistry, Virginia Polytechnic Institute and State University, Blacksburg, Virginia 24061-0344

Received September 7, 1995. Revised Manuscript Received November 15, 1995⊗

This paper describes the structure/property relationships including the polymer backbone structures and molecular weight, chromophore/polymer interactions, and chromophore functionalization that influence the chromophore orientational dynamics and polymer relaxations in a special class of thermally stable polymers that was recently developed for second-order nonlinear optical applications. These poly(arylene ether) polymers (synthesis and characterization reported elsewhere) are being investigated because of their high glass transition temperatures (>200 °C), which may minimize the randomization of chromophore orientation following electric field poling. They also have hydrogen-bonding sites that can interact with the chromophores, which may improve the temporal stability of chromophore orientation following poling. Generalization of the observed polymer dynamics to other second-order nonlinear optical polymers is discussed. Second harmonic generation, a second-order nonlinear optical effect, and dielectric relaxation are the two techniques employed to examine the intermolecular cooperativity and segmental relaxation behavior in these polymers. By examination of the second-order nonlinear optical properties of the doped or functionalized polymeric material as a function of time and temperature and the dielectric relaxation phenomena as a function of frequency and temperature, information concerning the local mobility and relaxation phenomena of the polymer microenvironment surrounding the nonlinear optical chromophores can be obtained. The dielectric loss data were analyzed using the Havriliak−Negami empirical function and the Schonhals and Schlosser model to examine the extent of intermolecular coupling in these polymer systems. Results obtained using these two techniques are correlated.

Introduction

Over the past decade, researchers have been actively involved in developing novel polymeric materials with large nonlinear optical (NLO) responses for device applications.[1] Although current polymers have sufficient second-order NLO signal, they are not yet practical for device applications because of limitations in the temporal and thermal stability of chromophore orientation following electric field poling. This is caused by poor thermal stability of the polymer hosts, many of which soften and allow chromophore disorientation at temperatures as low as 25 °C, whereas commercial and military applications require long-term optical stability at operating temperatures as high as 80−125 °C and at processing temperatures that may exceed 250 °C.[2]

Most of the recent research mainly focus on synthesizing polymers with high glass transition temperatures, T_g's, and rigid backbones that would minimize the randomization of chromophore orientation following poling, improving the optical stability.[3] Several elegant approaches have been used to optimize polymer structures to maximize stability.[3] However, the studies of the polymer physics of these high-temperature stable polymeric materials are still incomplete, and general guidelines for optimizing the structures have not been formulated. It is critical to understand the polymer physics governing the relaxation behavior of these NLO

* To whom correspondence should be addressed.
† Present address: Applied Materials, Santa Clara, CA 95050.
‡ Present address: Bayer, Inc., Pittsburgh, PA 15205.
⊗ Abstract published in *Advance ACS Abstracts,* January 1, 1996.

(1) Prasad, P. N.; Williams, D. J. *Introduction to Nonlinear Optical Effects in Molecules and Polymers*; John Wiley & Sons, Inc.: New York, 1991.

(2) (a) Wu, J. W.; Binkley, E. S.; Kenney, J. T.; Lytel, R.; Garito, A. F. *J. Appl. Phys.* **1991**, *69*, 7366. (b) Lytel, R.; Lipscomb, G. F.; Binkley, E. S.; Kenney, J. T.; Ticknor, A. J. In *Materials for Nonlinear Optics: Chemical Perspectives*; Marder, S. R., Sohn, J. E., Stucky, G. D., Eds.; ACS Symposium Series 455; American Chemical Society: Washington, DC, 1991.

(3) (a) Wu, J. W.; Valley, J. F.; Ermer, S.; Binkley, E. S.; Kenney, J. T.; Lipscomb, G. F.; Lytel, R. *Appl. Phys. Lett.* **1991**, *58*, 225. (b) Wu, J. W.; Valley, J. F.; Ermer, S.; Binkley, E. S.; Kenney, J. T.; Lytel, R. *Appl. Phys. Lett.* **1991**, *59*, 2213. (c) Stahelin, M.; Burland, D. M.; Ebert, M.; Miller, R. D.; Smith, B. A.; Twieg, R. J.; Volksen, W.; Walsh, C. A. *Appl. Phys. Lett.* **1992**, *61*, 1626. (d) Xu, C.; Wu, B.; Dalton, L. R.; Shi, Y.; Ranon, P. M.; Steier, W. H. *Macromolecules* **1992**, *25*, 6714. (e) Yu, L.; Chan, W.; Dikshit, S.; Bao, Z.; Shi, Y.; Steier, W. H. *Appl. Phys. Lett.* **1992**, *60*, 1655. (f) Chen, J. I.; Marturunkakul, S.; Li, L.; Jeng, R. J.; Kumar, J.; Tripathy, S. K. *Macromolecules* **1993**, *26*, 7379. (g) Tapolsky, G.; Lecomte, J. P.; Meyrueix, R. *Macromolecules* **1993**, *26*, 7383. (h) Peng, Z.; Yu, L. *Macromolecules* **1994**, *27*, 2638. (i) Weder, C.; Neuenschwander, P.; Suter, U. W.; Pretre, P.; Kaatz, P.; Gunter, P. *Macromolecules* **1994**, *27*, 2181. (j) Yu, D.; Gharavi, A.; Yu, L. *Appl. Phys. Lett.* **1995**, *66*, 1050.

0897-4756/96/2808-0514$12.00/0

polymeric materials so that one can better predict the long-term thermal and temporal stability and changes in properties throughout the anticipated service life when utilizing them for optical device applications. The goal of this work is to investigate the structure/property relationships that influence the segmental relaxations of a special class of recently developed NLO polymers.

The class of polymers being investigated is polyarylene ethers.[4] These polymers are of interest for second-order NLO applications because of their high T_g's (>200 °C), which are comparable to many high-temperature polyimides, and because we can tailor the backbone structure to controllably manipulate the relative stiffness. The purity of these polymers is high, so that little of the impurities typically found in commercial materials can interfere with the measurement of second-order NLO properties. They also have hydrogen-bonding sites that can interact with the chromophores, which may improve the temporal stability of chromophore orientation following poling. 4-Amino-4′-nitroazobenzene (disperse orange 3, DO3) and 4-(dimethylamino)-4′-nitrostilbene (DANS) were chosen as the NLO chromophores for this study because both have high melting temperatures and similar structures. They also have similar sizes (approximately 200 Å^3) so that the effect of differing chromophore sizes on the dopant orientational dynamics is minimal.[5] Furthermore, the former chromophore is capable of hydrogen bonding via the terminal amine moiety, whereas the latter one is not. They are thus suitable for studying the effect of chromophore/polymer interactions on the dopant orientational dynamics in these guest−host systems.

Some progress had been made to improve the temporal stability of chromophore orientation following poling by covalently bonding the chromophores to the polymer backbone via hydrogen-bonded networks or by employing chromophores that could hydrogen bond to the polymer. Marks and co-workers observed a considerable reduction of the loss of second harmonic signal following poling in the poly(*p*-hydroxystyrene)-*N*-(4-nitrophenyl)-(*S*)-prolinol chromophore-functionalized polymer system.[6] This was achieved because of the restricted chromophore mobility imparted by covalent linkage to the polymer backbone and by the hydrogen-bonded networks. The effect of hydrogen bonding on the temporal stability of doped poly(methyl methacrylate) (PMMA) systems was investigated by employing one chromophore that could hydrogen bond to the polymer backbone and one that could not.[7] Improved temporal stability at temperatures near and above T_g was observed in the hydrogen-bonded system. However, the T_g's of these systems were below 150 °C, which were not yet high enough for device requirements.

To examine the relaxation behavior in these thermally stable polymers, second harmonic generation and dielectric relaxation are the two techniques employed. Second harmonic generation, a second-order NLO technique, is sensitive to small degrees of chromophore rotational mobility. The initial local free volume surrounding the chromophores changes with time in the local glassy microenvironment, affecting the second harmonic intensity. Electric field-induced chromophore orientation occurs in regions of sufficient local free volume and segmental mobility. The disorientation of the chromophores is caused by mobility of the polymer chains and local free volume present in the vicinity of the chromophores; the relaxations of the polymer chains and the presence of local free volume prevent the "freezing in" of the imposed orientation. Chromophore orientation can thus be examined over a wide range of time and temperature scales as a function of the local free volume and segmental mobility in the glassy polymer matrix. Dielectric relaxation has been shown to be a useful technique for studying the transitions, relaxations, and intra- and intermolecular interactions in polymeric materials.[8−10] In this study, it is employed to examine the intermolecular cooperativity and segmental relaxations in the homo-, doped and functionalized polymer systems.

The experiments discussed in this paper evaluate the effects of polymer backbone structures and molecular weight, chromophore/polymer interactions, and chromophore functionalization on dopant orientational dynamics and polymer relaxations in these thermally stable polymers. By examination of the second-order NLO properties of the doped or functionalized polymeric material as a function of time and temperature and the dielectric relaxation phenomena as a function of frequency and temperature, information concerning the local mobility and relaxation phenomena of the polymer microenvironment surrounding the NLO chromophores can be obtained. Information obtained for this particular class of materials should prove to hold for other classes of related high-temperature stable materials for second-order nonlinear optical applications.

Background

Second-Order Nonlinear Optics. The principles of second-order nonlinear optics are briefly outlined here. A complete development is available elsewhere.[1,11,12] Second harmonic generation (SHG) is a special case of frequency mixing occurring when light waves of frequency ω passing through an array of molecules interact with them in such a way as to produce light waves at double the original frequency. It arises from the second-order NLO susceptibility $\chi^{(2)}$ tensor found in the expansion of bulk polarization, P, in powers of field strength, E:[13]

$$P = \chi^{(1)}\cdot E + \chi^{(2)}:EE + \chi^{(3)}:EEE + \ldots \qquad (1)$$

where $\chi^{(1)}$, $\chi^{(2)}$, and $\chi^{(3)}$ are linear and second- and third-order susceptibility tensors relating the bulk polarization, P, to the field strength, E. Since SHG effect, a result of the second-order polarization, is proportional to the optical field squared, $\chi^{(2)}$ is zero in a centrosym-

(4) Priddy, Jr., D. B.; Fu, C. Y. S.; Pickering, T. L.; Lackritz, H. S.; McGrath, J. E. *Mater. Res. Soc. Symp. Proc.* **1993**, *328*, 589.
(5) Hampsch, H. L.; Yang, J.; Wong, G. K.; Torkelson, J. M. *Polym. Commun.* **1989**, *30*, 40.
(6) (a) Ye, C.; Minami, N.; Marks, T. J.; Yang, J.; Wong, G. K. *Macromolecules* **1988**, *21*, 2899. (b) Jin, Y.; Carr, S. H.; Marks, T. J.; Lin, W.; Wong, G. K. *Chem. Mater.* **1992**, *4*, 963.
(7) Hampsch, H. L.; Yang, J.; Wong, G. K.; Torkelson, J. M. *J. Polym. Sci., Polym. Lett.*, in press.
(8) Rellick, G. S.; Runt, J. *J. Polym. Sci.: Polym. Phys. Ed.* **1986**, *24*, 313.
(9) Lei, D.; Runt, J.; Safari, A.; Newnham, R. E. *Macromolecules* **1987**, *20*, 1797.
(10) Ngai, K. L.; Roland, C. M. *Macromolecules* **1993**, *26*, 6824.
(11) Bloembergen, N. *Nonlinear Optics*; W. A. Benjamin, Inc.: New York, 1965.
(12) Shen, Y. R. *The Principles of Nonlinear Optics*; John Wiley & Sons, Inc.: New York, 1984.

metric or randomly oriented medium due to cancellation of the net dipole moment. To make a material capable of SHG effect, NLO chromophores must therefore be oriented noncentrosymmetrically in the polymer matrix[13,14] which can be achieved by corona poling.

Corona poling[15] creates an electric field by generating a discharge from a metallic needle tip. Because of the high field generated, the surrounding air becomes ionized with the same polarity as the corona discharge. These ions are driven toward and deposited onto the polymer film surface creating a field high enough to orient the chromophores, generating a second harmonic signal. When the applied voltage is turned off, chromophores in regions of sufficient mobility rotate out of the poling induced orientation, no longer contributing to the second harmonic intensity. By following the decay of the signal, the temporal stability of chromophore orientation can be examined. It must be noted that residual surface and space charges persist in the films following corona poling,[15b] which complicates the analyses of relaxation data. Polymer relaxations and residual charge effects must both be considered when evaluating the dopant orientational dynamics, and no *absolute* measure of the relaxation time of the chromophores can be determined. Several researchers have assumed the effects were negligible at low corona fields, whereas others, including our work, have tried to measure these effects directly.[15b,c] The electric field effects in this case are poorly understood and a topic of much ongoing research.[15d,16] A surface voltage probe has been used to measure the surface voltage decay following poling in the doped PMMA systems.[23b] However, because the probe of the electrostatic voltmeter that we are using cannot withstand temperatures greater than 50 °C, surface voltage measurements could not be performed on these polymers. A high temperature stable probe is under design. This work thus focuses on aspects of polymer relaxations and all relaxation data reported here using second harmonic generation include electric field effects, as is done by many researchers in the field. Note that near T_g these effects are relatively short lived (in PMMA doped with DANS at T_g, the residual field persisted for less than an hour[23c]), but they are still significant. The SHG decay data thus obtained, however, allow one to qualitatively interpret trends in the temporal stability of dopant orientation following poling.

For SHG in this geometry, $\chi^{(2)}_{333}$ and $\chi^{(2)}_{311}$ are the only two nonzero susceptibility tensors, and $\chi^{(2)}_{311} \approx {}^1/_3\,\chi^{(2)}_{333}$ in the limit of low poling field. The expression for $\chi^{(2)}_{333}$ is given by[17]

$$\chi^{(2)}_{333} \approx N f_3^2(\omega)\, f_3(2\omega) \beta_{zzz} \langle \cos^3 \theta \rangle \qquad (2)$$

where N is the number of molecules per unit volume and $f_i(\Omega)$ is the local field factor at frequency Ω for fields polarized along the i direction.[18] The subscript 3 refers to the direction of the orienting (poling) field and z denotes the axis of the molecule parallel to the molecular dipole moment. The angle between 3 and z directions is represented by θ, and $\langle \cos^3 \theta \rangle$ is the average of $\cos^3 \theta$ over the ensemble. β_{zzz} is the second-order hyperpolarizability along the longest axis of the molecule and is assumed to be roughly equal to β of the molecule ($\beta = \beta_{zxx} + \beta_{zyy} + \beta_{zzz}$).

Dielectric Relaxation. The basic theory of dielectric relaxation has been extensively covered elsewhere.[19] Here, the dielectric dispersion phenomena[20a,b] and the Havriliak−Negami equation[20a] and the Schonhals and Schlosser model[21] that have been used to describe the loss curves in polymers are briefly outlined. Two types of dielectric experiments have been performed.[19] A sample can be held at a constant temperature while the frequency is scanned or it is held at constant frequency while the temperature is varied. In both constant-temperature and constant-frequency experiments, dispersion is depicted by a peak in ϵ'' or tan δ_ϵ (dissipation) which indicates that some forms of dipolar molecular motions are taking place. These motions can be associated to the micro-Brownian motion of the polymer main chain (α relaxation) or motions of the flexible side groups along the chain (β relaxation).

The Havriliak−Negami empirical function has been extensively used to describe the breadth and asymmetry of the dielectric loss curves in polymers.[20a] Havriliak and Negami (H−N) found that the relaxation process can be represented as the sum of two dispersions, and proposed an empirical expression to represent the data:

$$\frac{\epsilon^*(\omega) - \epsilon_\infty}{\epsilon_0 - \epsilon_\infty} - \frac{1}{[1 + (i\omega\tau_0)^\alpha]^\beta} \qquad (3)$$

where ϵ_0 and ϵ_∞ are the relaxed and unrelaxed relative permittivities (as defined by H−N[20a]), respectively, and τ_0 is the characteristic relaxation time. The parameter α represents the symmetric broadening of the dielectric loss curve, and β is correlated to the asymmetric nature of the dispersion curve. α and β are able to vary between $0 < \alpha \leq 1$ and $0 < \beta \leq 1$.

Because the Havriliak−Negami function is a phenomenological relationship, a model was later developed by Schonhals and Schlosser in order to better relate the fitting parameters α and β to the structures of polymers.[21] In this model, the frequency dependence of dielectric loss factor in the low-frequency limit was scaled as $\epsilon''(\omega) \propto \omega^\alpha$ for $\omega \ll \tau_0^{-1}$ and in the high-frequency limit, $\epsilon''(\omega) \propto \omega^{-\alpha\beta}$ for $\omega \gg \tau_0^{-1}$. Thus, on a

(13) *Nonlinear Optical Properties of Organic and Polymeric Materials*; Williams, D. J., Ed.; ACS Symposium Series 233; American Chemical Society: Washington, DC, 1983.

(14) *Nonlinear Optical Properties of Organic Molecules and Crystals*; Chemla, D. S.; Zyss, J., Eds.; Academic Press, Inc.: New York, 1987; Vols 1 and 2.

(15) (a) *Electrets*; Sessler, G. M., Ed.; Springer-Verlag: Berlin, Germany, 1980. (b) Hampsch, H. L.; Torkelson, J. M.; Bethke, S. J.; Grubb, S. G. *J. Appl. Phys.* **1990**, *67*, 1037. (c) Giacometti, J. A.; Oliveira, Jr., O. N. *IEEE Transactions on Electrical Insulation* **1992**, *27*, 924. (d) Pasmore, T.; Talbot, J.; Lackritz, H. S. *Nonlinear Optics*, in press. Lackritz, H. S.; Liu, L. Y.; Ostrowski, M. H., manuscript in preparation.

(16) (a) Haber, K. S.; Ostrowski, M. H.; O'Sickey, M. J.; Lackritz, H. S. *Mater. Res. Soc. Symp. Proc.* **1994**, *328*, 547. (b) Ghebremichael, F.; Lackritz, H. S. *J. Appl. Phys.*, submitted.

(17) (a) Singer, K. D.; Kuzyk, M. G.; Sohn, J. E. *J. Opt. Soc. Am. B* **1987**, *4*, 968. (b) Boyd, G. T.; Francis, C. V.; Trend, J. E.; Ender, D. A. *J. Opt. Soc. Am. B.* **1991**, *8*, 887.

(18) Onsager, L. *J. Am. Chem. Soc.* **1936**, *58*, 1486.

(19) (a) McCrum, N. G.; Read, B. E.; Williams, G. *Anelastic and Dielectric Effects in Polymeric Solids*; John Wiley & Sons Ltd.: London, 1967. (b) Pochan, J. M.; Pai, D. M. Dielectric and Photoconductive Properties. In *Plastics Polymer Science and Technology*; Baijal, M. D., Ed.; Wiley-Interscience: New York, 1982.

(20) (a) Havriliak, S.; Negami, S. *J. Polym. Sci.: Part C* **1966**, *14*, 99. (b) Jonscher, A. K. *Dielectric Relaxation in Solids*; Chelsea Dielectrics Press Ltd.: London, 1983. Jonscher, A. K. Dielectric Response of Polar Materials. *IEEE Trans. Electron. Insul.* **1990**, *25*, 622.

(21) Schonhals, A.; Schlosser, E. *Colloid Polym. Sci.* **1989**, *267*, 125; **1989**, *267*, 133.

Table 1. Structures and Thermal and Physical Characterization Data of the Host Polymers

polymer	T_g (°C)	TGA (°C) 5% wt loss in air	$\bar{M}_w$ (g/mol)	$\bar{M}_n$ (g/mol)
Bis A-PEPO 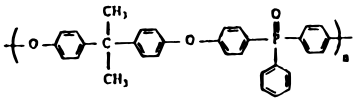	210	490	30,000	15,000
F_6 Bis A-PEPO 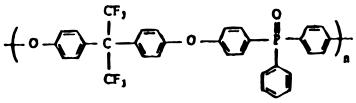	265	500	35,660	18,130
PP-PEPO 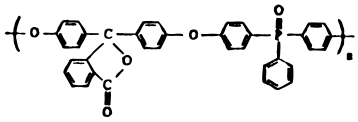	259	496	32,200	16,100
PP-PES 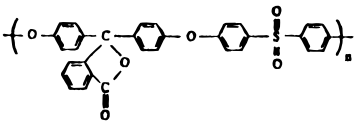	226	490	31,000	15,500
PP-PEK 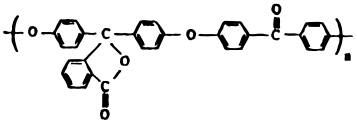	284	490	32,000	16,000
PP-PEPO-pNPH 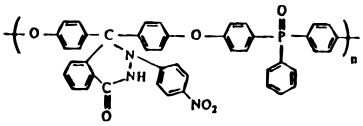	278	485	30,000	15,000
PP-PEPO-DNPH 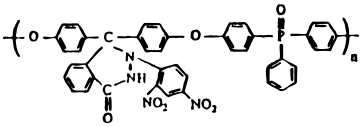		485	30,000	15,000

log−log plot of the dielectric loss factors as a function of frequency (as first plotted by Jonscher,[20b] who used this type of plot to understand the physical nature of loss within an energy, screened polarization, and mechanical relaxation formalism), the slope of the dielectric loss peak on the low-frequency side ($\omega\tau_0 \ll 1$) is proportional to α, while it is proportional to $-\alpha\beta$ on the high-frequency side ($\omega\tau_0 \gg 1$). The parameter α is correlated with the intermolecular dynamics, while the product $\alpha\beta$ describes the local intramolecular dynamics of the polymer. Furthermore, α decreases in the range $1 > \alpha > 0$ with increasing large-scale correlation of the segments of different chains, and $\alpha\beta$ decreases in the range $0.5 > \alpha\beta > 0$ with an increase of hindrance of the local segments. In this research, the Havriliak−Negami equation and the Schonhals and Schlosser model are employed to determine the values of α and β and to evaluate the extent of intermolecular coupling arising from various steric interferences of the polymer backbones and chromophore/polymer interactions.

Experimental Techniques

This section describes the experimental protocols employed to investigate the relaxation phenomena in the homo-, doped, and side-chain functionalized polyarylene ether polymers.

Material Preparation and Characterization. The amorphous, thermally stable poly(arylene ether) polymers synthesized by McGrath and co-workers[4] are investigated. The structures and properties of these homo- and side-chain functionalized polymers, Bis A−poly(arylene ether) phosphine oxides (PEPO), F_6 Bis A−PEPO, phenolphthalein−PEPO (PP−PEPO), phenolphthalein−poly(arylene ether) ketone (PP−PEK), phenolphthalein−poly(arylene ether) sulfone (PP−PES), PP−PEPO derivatized with 10% *p*-nitrophenylhydrazine (PP−PEPO−pNPH), and PP−PEPO derivatized with 10% 2,4-dinitrophenylhydrazine (PP−PEPO−DNPH), are shown in Table 1. Detailed synthesis and characterization of these polymers can be found elsewhere.[4] All of the polyarylene ethers investigated here have number average molecular weight, $\bar{M}_n$, of 15 000 g/mol and polydispersity indexes of approximately 2. PP−PEPO and $\bar{M}_n$ of 41 000 g/mol and polydispersity index of approximately 2 was also investigated.

The structures and properties of the two NLO chromophores, 4-(dimethylamino)-4′-nitrostilbene (DANS, Kodak) and 4-amino-4′-nitroazobenzene (disperse orange 3, DO3, Aldrich, 95% pure), used in this study are shown in Table 2. DANS was used as received. DO3 was further purified via recrystallization with acetone. DANS and DO3 chromophores induce slight resonance enhancement in the measured values for $\chi^{(2)}$ at 1064 nm; thus all data are modified by a constant value and no absolute values for the second harmonic intensity are reported. This does not affect the conclusions reached below in any fashion.

Table 2. Structures and Thermal and Physical Characterization Data of the Nonlinear Optical Chromophores

chromophore	T_m (°C)	MW (g/mol)	V (Å^3)[a]
4-amino-4'-nitroazobenzene (disperse orange 3, DO3) 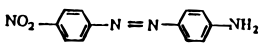	215	242.2	179
4-dimethylamino-4'-nitrostilbene (DANS) 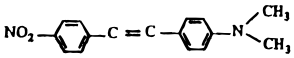	256	268.3	206

[a] Volume calculated using van der Waals volumes.[34]

Polymer and 10 wt % chromophore were dissolved in chloroform ($CHCl_3$) to make up a solution that contained about 10 wt % solids. This solution was well mixed, filtered through a 5 μm filter, and spin-coated onto indium tin oxide (ITO) coated glass slides. The spun films were then dried to remove as much solvent as possible. They were first dried at ambient conditions for about 48 h and then under vacuum for about 24 h at ambient temperature and heated slowly over 1 day to approximately T_g + 10 °C. They were then slowly cooled to 25 °C and stored in a desiccator before SHG measurements were performed.

Samples for dielectric relaxation experiments were prepared by spin-coating the undoped or doped polymers onto 50:50 ITO:glass substrates.[22] After careful drying, gold electrodes were then deposited on top of the films using an evaporator.

Film thicknesses measured via profilometry ranged between 4 and 6 μm for SHG measurements and between 12 and 20 μm for dielectric relaxation experiments. The absorbances of the undoped polymers obtained from the ultraviolet and visible spectroscopy were between 200 and 300 nm and those of the DO3- and DANS-doped polymeric films were between 350 and 550 nm. The T_g's of the undoped and doped materials were measured via differential scanning calorimetry (DSC, 10 °C/min heating rate).

Second Harmonic Generation Apparatus and Experiments. The detailed descriptions of the SHG and corona poling apparatus can be found elsewhere.[23] The laser light was generated by a Q-switched Nd:YAG laser (10 Hz, 6−8 ns pulse width) at a fundamental wavelength of 1.064 μm. The beam was p-polarized and split so that the sample and quartz (or 2-methyl-4-nitroaniline, MNA) reference could be tested simultaneously. The polymer film was heated to T_g + 5 °C in approximately 20 min and maintained at this temperature for 1 h to ensure uniform thermal history. The voltage was then applied for 25 min at this temperature and remained on until the film was cooled to the temperature at which the randomization of chromophore orientation was to be observed. The voltage was turned off once the final temperature was reached. The randomization of chromophore orientation was then observed at this temperature. It is more difficult to orient chromophores when the films are poled below T_g because of the restricted segmental mobility that hinders rotation.[24] All of the films were thus poled above T_g in order to enhance the second harmonic signal during poling and achieve better temporal stability of chromophore orientation following poling. The films were cooled from above to below T_g during poling because the local free volume in the matrix decreases around the oriented chromophores, restricting their mobility. The $\chi^{(2)}$ values of the samples were ratioed to those of quartz (or MNA) reference to minimize errors due to laser drifts and/or changes in the ambient environment and then normalized to the point at which the applied voltage was turned off. The errors due to noise in these reported $\chi^{(2)}$ values were less than or equal to twice the size of the symbols.

Dielectric Relaxation Apparatus and Experiments. Dielectric relaxation experiments were performed with GenRad 1689 RLC Digibridge, with a frequency range between 12 Hz and 100 kHz and a frequency tolerance of 0.005%. One volt peak-to-peak was used for all experiments. A convection oven (Delta Design 9023) with an accuracy of ±0.1 °C was used to control the temperature during the measurements. The Digibridge and oven were interfaced with a Macintosh Quadra 950 and remote controlled using the LabView program.

For each dielectric experiment, the film was heated to approximately T_g − 100 °C in 8−10 min and maintained at this temperature for half an hour. The capacitance and tan δ_ϵ were then measured at 40 different frequencies between 12 Hz and 100 kHz. Values of capacitance and tan δ_ϵ at each frequency were averaged over 10 measurements. From the capacitance and tan δ_ϵ measured, ϵ' and ϵ'' were then calculated.[19,25] The procedure was repeated for temperatures every 10 °C up to approximately T_g + 50 °C. The dielectric values obtained from these experiments had a systematic error of ~5% which was mainly caused by the uncertainties in the measurements of the geometrical dimensions of the film thicknesses and electrodes.

Fourier Transform Infrared (FTIR) Spectroscopy. The transmission FTIR spectra were obtained using the Nicolet 800 FTIR spectrometer. The instrument was continually purged with dry air during the experiments to reduce water vapor and carbon dioxide in the sample chamber. The unpolarized incident beam had a resolution of 4 cm^{-1} and 256 scans were collected. The undoped and doped polymer samples were spin-coated onto potassium bromide plates for the measurements.

Results and Discussions

In this section, the intermolecular cooperativity and segmental relaxations arising from polymer backbone structures and molecular weight, chromophore/polymer interactions, and chromophore functionalization in these polyarylene ethers studied using SHG and dielectric relaxation are discussed.

Effect of Polymer Backbone Structures. Because the polymers investigated here had very similar backbones, with variations on a particular pendant group, the effect of backbone structures and steric constraints on the intermolecular cooperativity and segmental relaxation behavior could be examined. The variations in the breadth of the dielectric loss curves reflect differences in the distributions of relaxation times and changes in local microenvironment and inter- and intramolecular interactions.[8,10] A broadening on the low-frequency side of the loss curve was observed when the polymer backbone became more polar and/or sterically hindered, indicating that the intermolecular coupling became stronger. It should also be noted that under these experimental conditions, no β-transition was observed in any of these polyarylene ethers.

Figure 1 shows the normalized dielectric loss curves ($\epsilon''/\epsilon''_{max}$ vs f/f_{max}, where f_{max} is the frequency of peak maximum) for the undoped Bis A−PEPO, F_6 Bis A−PEPO, and PP−PEPO at a temperature of approximately T_g + 15 °C. The breadth of the dispersion curves increased in the order Bis A−PEPO < PP−PEPO < F_6 Bis A−PEPO, particularly on the low-frequency side of the loss peaks. Steric effects arising from the pendant fluorine atoms and the strong intermolecular interac-

(22) Kohler, W.; Robello, D. R.; Dao, P. T.; Willand, C. S.; Williams, D. J. *J. Chem. Phys.* **1990**, *93*, 9157.

(23) (a) Wright, M. E.; Mullick, S.; Lackritz, H. S.; Liu, L. Y. *Macromolecules* **1994**, *27*, 3009. (b) Liu, L. Y.; Ramkrishna, D.; Lackritz, H. S. *Macromolecules* **1994**, *27*, 5987. (c) Hampsch, H. L. Ph.D. Thesis, Northwestern University, 1990.

(24) Hampsch, H. L.; Yang, J.; Wong, G. K.; Torkelson, J. M. *Macromolecules* **1990**, *23*, 3640.

(25) Aklonis, J. J.; MacKnight, W. J. Dielectric Relaxation. In *Introduction to Polymer Viscoelasticity*, 2nd ed.; John Wiley and Sons, Inc.: New York, 1983; pp 189−211.

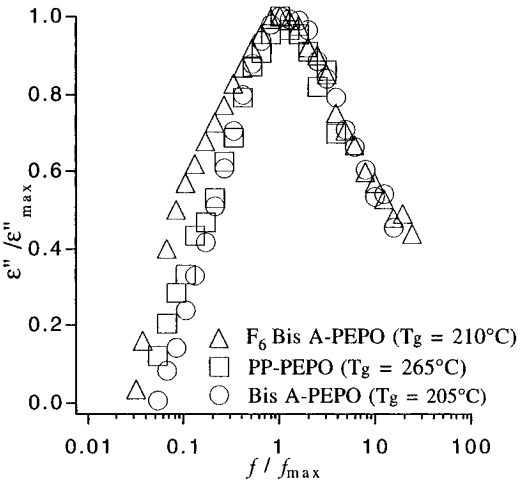

Figure 1. $\epsilon''/\epsilon''_{max}$ vs f/f_{max} for undoped Bis A−PEPO, F_6 Bis A−PEPO, and PP−PEPO measured at T_g + 15 °C.

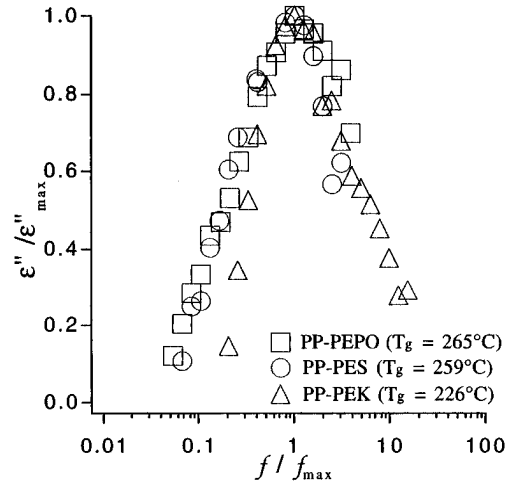

Figure 2. $\epsilon''/\epsilon''_{max}$ vs f/f_{max} for undoped PP−PEPO, PP−PES, and PP−PEK measured at T_g + 15 °C.

tions associated with their high electronegativity in F_6 Bis A−PEPO resulted in the broadest loss curve. This showed that F_6 Bis A−PEPO exhibited the strongest intermolecular coupling. PP−PEPO, because of its bulky heterocyclic pendant lactone, resulted in a slightly broader dispersion curve than that of Bis A−PEPO. However, because the heterocyclic pendant lactone on PP−PEPO was not as polar as the fluorine atoms on F_6 Bis A−PEPO, it may not be as intermolecularly coupled as reflected by the narrower loss curve. Similar trends were also observed in the normalized loss curves for the undoped PP−PEPO, PP−PES, and PP−PEK as shown in Figure 2. The phosphine oxide functionality on PP−PEPO was more bulky than the ketone functionality on PP−PEK and the sulfone functionality on PP−PES, resulting in the broadest loss curve. Furthermore, the sulfone functionality on PP−PES was more bulky than the ketone functionality on PP−PEK, resulting in the broader dispersion curve. These results were consistent with those observed in the polymers with lower T_g's and more flexible backbones.[10] It has been reported that for polymers with smoother, less polar, and more flexible and symmetrical backbones, there is less constraint on segmental relaxations from interactions with neighboring, nonbonded segments, resulting in narrower dielectric loss curves, whereas those with stiffer backbones and/or sterically hindering pendant groups exhibit broader dispersion curves, reflecting broader distributions of relaxation times and stronger intermolecular coupling.[10]

Table 3. Values of α and αβ Obtained from the Havriliak−Negami Equation Fit

polymer	α	αβ
Bis A−PEPO	0.95 ± 0.02	0.45 ± 0.23
F_6 Bis A−PEPO	0.81 ± 0.03	0.38 ± 0.21
PP−PEPO	0.88 ± 0.04	0.51 ± 0.28
PP−PES	0.96 ± 0.05	0.64 ± 0.22
PP−PEK	0.99 ± 0.05	0.64 ± 0.26
PP−PEPO−pNPH	0.73 ± 0.03	0.72 ± 0.22
PP−PEPO−DNPH	0.77 ± 0.03	0.76 ± 0.21

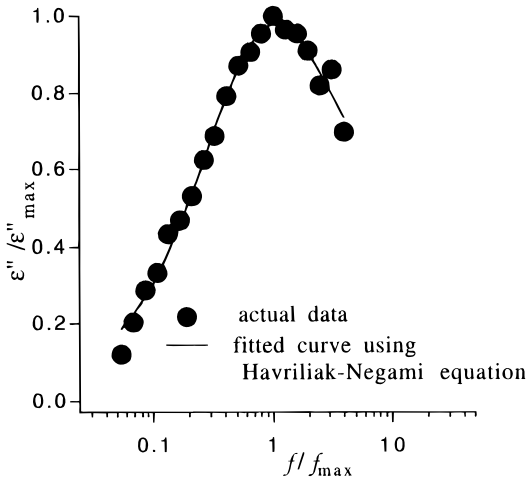

Figure 3. $\epsilon''/\epsilon''_{max}$ vs f/f_{max} for undoped PP−PEPO measured at T_g + 15 °C. The solid curve is the Havriliak−Negami equation fit.

It must be noted that the differences in the breadth of the loss curves obtained for the polyarylene ethers investigated here were small because these polymers were very structurally similar. Similar phenomena were also observed in the polymers with lower T_g's and more flexible backbones.[10] Furthermore, when comparing this traditional characterization method with SHG, the former technique is less sensitive to changes in local microenvironment.

The Havriliak−Negami equation and the Schonhals and Schlosser model were used to fit and describe these dielectric loss curves. The equation was able to fit them well and the results of the fits are reported in Table 3. Figure 3 shows the fit to the dispersion curve of the PP−PEPO polymer. For Bis A−PEPO, F_6 Bis A−PEPO, and PP−PEPO, the value of α was the smallest for F_6 Bis A−PEPO, indicating that it had the strongest intermolecular coupling. Similarly, for PP−PEPO, PP−PES, and PP−PEK, the value of α was the smallest for PP−PEPO, again indicating that it had the strongest intermolecular cooperativity. This was the first attempt, as far as we know, to employ the Schonhals and Schlosser model to describe the extent of intermolecular interactions arising from various steric interferences, and as shown here the model can successfully correlate the values of α to the intermolecular coupling of these polymers.

Second harmonic generation experiments were also performed on the DO3 doped Bis A−PEPO, F_6 Bis A−PEPO, and PP−PEPO systems, and the results are shown in Figure 4. The temporal stability of chromophore orientation at T_g − 140 °C following poling increased in the order Bis A−PEPO < PP−PEPO < F_6 Bis A−PEPO. Because of the strongest intermolecular cooperativity of the F_6 Bis A−PEPO chain segments,

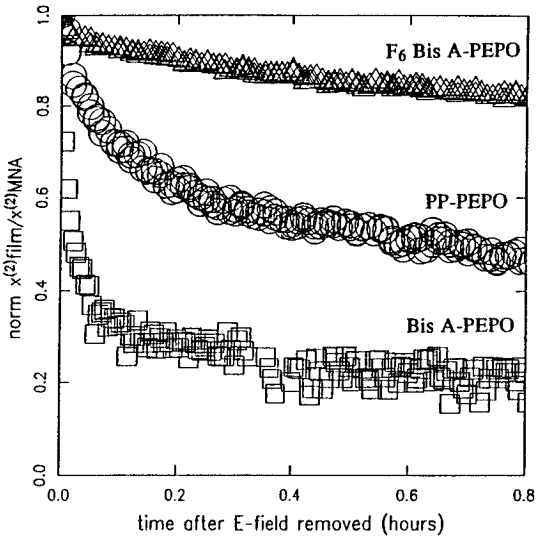

Figure 4. Temporal stability of chromophore orientation in Bis A−PEPO, F_6 Bis A−PEPO, and PP−PEPO doped with 10 wt % DO3 poled at T_g + 5 °C; temperature at which chromophore disorientation was observed ≈ T_g − 140 °C.

chromophore motions were strongly restricted, resulting in the most stable second harmonic signal. Since the PP−PEPO chain segments were not as intermolecularly coupled as F_6 Bis A−PEPO, chromophores could more easily rotate out of the poling induced orientation, resulting in the less stable second harmonic signal. The DO3-doped Bis A−PEPO system showed the poorest temporal stability of chromophore orientation because it was not as intermolecularly coupled as the F_6 Bis A−PEPO and PP−PEPO systems. This demonstrates that by combining dielectric relaxation and SHG, information concerning the extent of intermolecular coupling and local mobility in these polymer matrixes can be obtained.

It is difficult to directly compare the dielectric loss curves of the polymers investigated in this work with those that have more flexible backbones reported in the literature because of different molecular weight and polydispersities of the polymers. However, attempts were made here to compare the polymer systems that have similar structures or polydispersities. It must be noted that the dispersion curve for Bis A−PEPO reported here was at T_g + 15 °C. However, the data for this polymer were also taken up to T_g + 50 °C. When the normalized loss curves, a single master curve formed; that is, the breadth of the loss curves remained very similar as the temperature increased.

The normalized loss curves of the undoped Bis A−PEPO ($\bar{M}_n \approx 15\,000$ g/mol, $\bar{M}_w \approx 30\,000$ g/mol) investigated here and the undoped bisphenol A−polycarbonate (BPA−PC, $\bar{M}_n \approx 10\,000$ g/mol, $\bar{M}_w \approx 30\,000$ g/mol) reported by Ngai and co-workers[10,26] which have similar structures were compared. The temperature at which the normalized loss curve of BPA−PC was reported was not specifically stated in the paper.[10] However, it can be seen from the log [τ^*] vs T_g/T plot that the data for this polymer were taken from T_g to approximately T_g + 15 °C. The thermal histories at which the dielectric loss data for these two polymers were taken were thus similar. Assuming that the breadth of the loss curves remained similar as the temperature increased (since

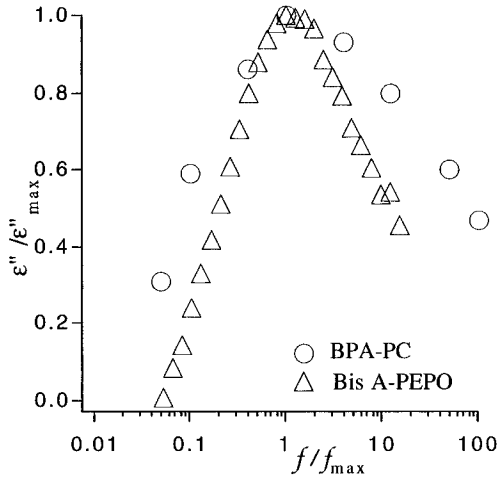

Figure 5. $\epsilon''/\epsilon''_{max}$ vs f/f_{max} for Bis A−PEPO ($\bar{M}_n \approx 15\,000$ g/mol, $\bar{M}_w \approx 30\,000$ g/mol; T_g = 205 °C) and BPA−PC ($\bar{M}_n \approx 10\,000$ g/mol, $\bar{M}_w \approx 30\,000$ g/mol; T_g = 150 °C) (reproduced with permission from ref 10).

it was not stated that the breadth varies with temperature[10]), the comparison of the breadth of these dispersion curves is legitimate. As shown in Figure 5, BPA−PC exhibited a broader loss curve than that of Bis A−PEPO, though the former polymer has less sterically hindered backbone. This result contradicted to reports in the literature and may be explained by the different polydispersities of the Bis A−PEPO and BPA−PC polymers.[26] It has been reported that for polydisperse polymers, the dispersion is inhomogeneously broadened because of the distribution of relaxation times; that is, the molecular weight distribution strongly affects the breadth of the loss curve, especially in the entangled regime.[27] Ngai and co-workers employed the coupling model to fit the shear loss moduli of BPA−PC that has a polydispersity index of about 3 and found a large discrepancy between the calculated and experimental data if an inhomogeneous distribution of primitive relaxation times was not included in the model.[27a] This supports the presence of an inhomogeneous distribution of relaxation times due to the molecular weight distribution in a polydisperse system. Adachi and Kotaka later reported that the dielectric loss curve for *cis*-polyisoprenes broadened significantly, particularly on the high-frequency side of the loss peak, when the polydispersity index increased from 1.08 to 1.34.[27b]

The normalized dispersion curve of the undoped Bis A−PEPO was also compared to that of the data taken by Torkelson and co-workers for poly(isobutyl methacrylate) (PIBMA, ($\bar{M}_n \approx 140\,000$ g/mol, $\bar{M}_w \approx 300\,000$ g/mol)[28] which has a more flexible backbone and polydispersity index similar to that of the Bis A−PEPO used here. The dielectric loss data of the 1 wt % 4-[*N*-ethyl-*N*-(2-hydroxyethyl)amino]-4′-nitroazobenzene (disperse red 1, DR1) doped PIBMA system were taken from T_g + 50 °C to T_g + 90 °C. It was pointed out that when the normalized loss curves were plotted, a single master curve with excellent overlap of the data formed, again indicating that the breadth of the loss curves remained unaltered as the temperature increased. The thermal histories at which the dielectric loss data for these two

(26) Yee, A. F.; Bankert, R. J.; Ngai, K. L.; Rendell, R. W. *J. Polym. Sci., Part B: Polym. Phys.* **1988**, *26*, 2463.

(27) (a) Ngai, K. L.; Rendell, R. W.; Yee, A. F. *Macromolecules* **1988**, *21*, 3396. (b) Adachi, K.; Kotaka, T. *Prog. Polym. Sci.* **1993**, *18*, 585.

(28) Dhinojwala, A.; Wong, G. K.; Torkelson, J. M. *Macromolecules* **1993**, *26*, 5943.

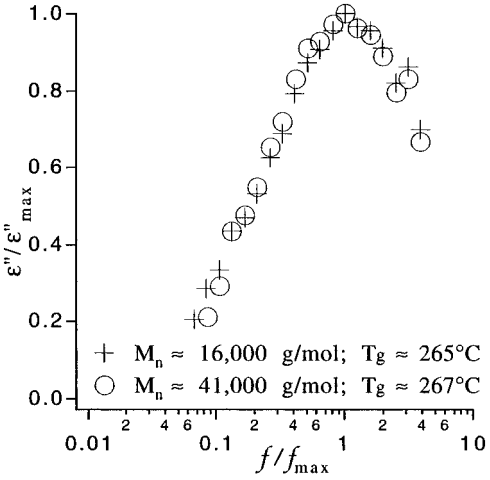

Figure 6. $\epsilon''/\epsilon''_{max}$ vs f/f_{max} for PP−PEPO with $\bar{M}_n$ of 41 000 g/mol and 16 000 g/mol measured at T_g + 15 °C.

polymers were taken were similar and the comparison of the breadth of the loss curves is thus legitimate. The breadth of the dispersion curve of the 1 wt % DR1-doped PIBMA system was very similar to that of Bis A−PEPO. One might expect that the undoped PIBMA would exhibit a slightly narrower loss curve than the 1 wt % DR1-doped PIBMA because of the weaker intermolecular coupling in the absence of chromophore/polymer interactions. It is also expected that the undoped PIBMA would exhibit a slightly narrower loss curve than Bis A−PEPO. This would agree with the literature in which polymers having stiffer backbones exhibit broader dispersion curves.[10] Again, these results are difficult to correlate because of different molecular weight and polydispersities of the polymers and experimental conditions; future experiments will attempt to generate data to further explain these observations.

Effect of Molecular Weight. Dielectric relaxation experiments were performed on the PP−PEPO polymers with $\bar{M}_n$ of 41 000 and 16 000 g/mol. As shown in Figure 6, both systems exhibited very similar loss curves. The molecular weight and T_g's of these polymers were measured using gel permeation chromatography and DSC, respectively.[4] The entanglement molecular weight was determined to be around 15 000 g/mol and above which the T_g was minimally affected. Similarity in the shape of the loss curves may be explained by this and the fact that the two polymers had similar polydispersities. This could indicate that these two polymers had similar distribution of relaxation times and the observed intermolecular cooperativity remained minimally affected in the molecular weight range examined.

Because of similar intermolecular coupling observed via dielectric relaxation, one would expect that these two systems exhibit similar temporal stability of chromophore orientation following poling. However, SHG experiments showed that the 10 wt % DANS-doped PP−PEPO system with $\bar{M}_n$ of 41 000 g/mol had better short-term temporal stability at T_g − 140 °C following poling than the sample with $\bar{M}_n$ of 16 000 g/mol (Figure 7a). The overall stability remained similar for both systems (Figure 7b). These phenomena may be explained by the following hypothesis: The better short-term temporal stability may be due to the fact that there was less chain-end density in the high-molecular-weight sample, creating less free volume for the chromophores that were in the vicinity of the chain ends to rotate out of

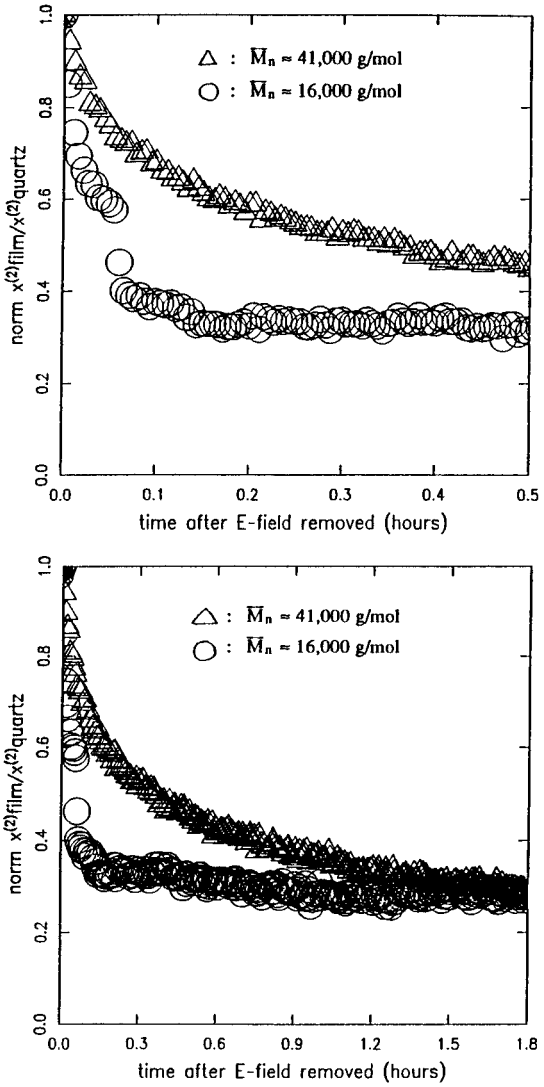

Figure 7. (a, top) Short-term and (b, bottom) overall temporal stability of chromophore orientation in 10 wt % DANS-doped PP−PEPO with $\bar{M}_n$ of 41 000 g/mol and 16 000 g/mol poled at −3500 V, T_g + 5 °C; temperature at which chromophore disorientation was observed ≈ T_g − 140 °C.

the poling-induced orientation. Since SHG is sensitive to changes in local microenvironment, a better short-term stability was observed in the high molecular weight system. However, the overall chromophore orientational dynamics was coupled to the polymer backbone motions. Since both systems were above the entangled level and had similar intermolecular coupling, the overall stability remained similar. To verify the above hypothesis, further experiments on the PP−PEPO systems with $\bar{M}_n$ between 16 000 and 41 000 g/mol will need to be performed to see if similar phenomena can be observed.

Effect of Chromophore/Polymer Interactions. The effect of chromophore/polymer interactions, specifically hydrogen bonding, on the chromophore orientational dynamics has been examined using SHG.[6,7] Here, this effect is investigated using SHG, dielectric relaxation, and FTIR spectroscopy. As shown in Figure 8, enhanced temporal stability of chromophore orientation at T_g − 140 °C following poling was clearly observed in the DO3-doped F_6 Bis A−PEPO matrix. The rotation of DANS is around the center of mass of the molecule because there is only dipole−dipole interactions between DANS and the polymer backbone. For the DO3 chro-

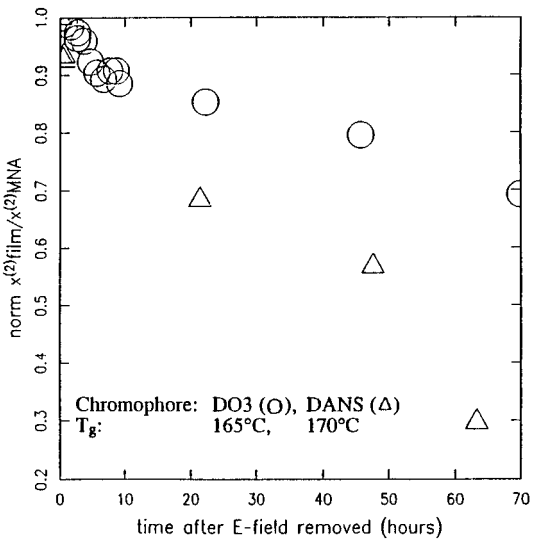

Figure 8. Effect of hydrogen bonding on the temporal stability of chromophore orientation in 10 wt % DO3 doped and 10 wt % DANS doped F_6 Bis A−PEPO systems poled at −3000 V, T_g + 5 °C; temperature at which chromophore disorientation was observed ≈ T_g − 140 °C.

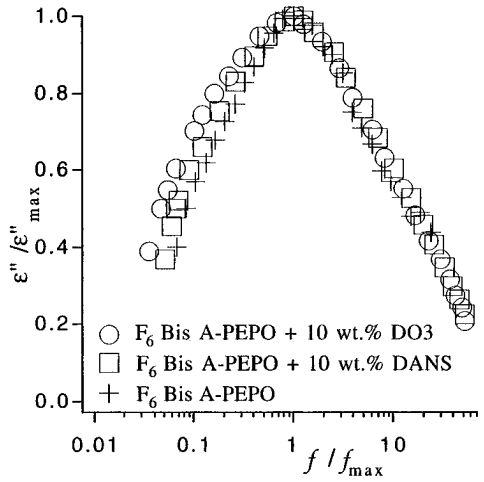

Figure 9. $\epsilon''/\epsilon''_{max}$ vs f/f_{max} for undoped F_6 Bis A−PEPO, 10 wt % DANS-doped F_6 Bis A−PEPO, and 10 wt % DO3-doped F_6 Bis A−PEPO measured at T_g + 15 °C.

mophore which can hydrogen bond to the polymer backbone, the rotation may be visualized as occurring around a fixed end point. It is clear that the DO3 chromophore will be more hindered in disorienting following poling because more free volume/local mobility is required for rotation; this then increasing the temporal stability of second harmonic signal following poling. This result is consistent with that observed in DO3- and DANS-doped PMMA systems.[7]

Dielectric relaxation experiments were also performed on the undoped, 10 wt % DANS-doped and 10 wt % DO3-doped F_6 Bis A−PEPO systems. Figure 9 shows the normalized loss curves for these three systems at a temperature of approximately T_g + 15 °C. The breadth of the dispersion curves increased in the order undoped F_6 Bis A−PEPO < 10 wt % DANS-doped F_6 Bis A−PEPO < 10 wt % DO3-doped F_6 Bis A−PEPO. This was because the intermolecular coupling should become stronger in the doped system, broadening the loss curve. The DO3-doped system resulted in a slightly broader dispersion curve than that of the DANS doped sample due to hydrogen bonding between DO3 and F_6 Bis A−PEPO, which further enhanced the intermolecular cooperativity. These results were consistent with those observed in polymers with lower T_g's and more flexible backbones such as the undoped and DR1-doped PMMA systems.[9]

FTIR spectra (from wavenumbers of 400 to 4000 cm^{-1}) were also obtained for the undoped, 10 wt % DANS-doped, and 10 wt % DO3-doped F_6 Bis A−PEPO systems. The spectra from 400 to 2000 cm^{-1} for these three samples were very similar and are not shown here. Figure 10 shows the FTIR spectra of these three systems from 2000 to 4000 cm^{-1}. The peak near 3060 cm^{-1} observed in all of these spectra was caused by the aromatic C−H stretching. The spectrum of the 10 wt % DO3-doped F_6 Bis A−PEPO system showed major difference in the 3200−3500 cm^{-1} region when compared with those of the undoped and 10 wt % DANS-doped F_6 Bis A−PEPO samples. Both the O−H (due to hydrogen bonding between DO3 and F_6 Bis A−PEPO) and chromophore N−H (DO3) stretching bands overlapped in this regime. The doublet near 3200 and 3300 cm^{-1} was caused by N−H stretching which was at slightly lower wavenumbers than that observed in the "free" N−H stretching. This was caused by hydrogen bonding between the chromophore and polymer, shifting the observed bands to lower wavenumbers.[29]

All of the three techniques used to study the hydrogen bonding effects showed consistent results. By combining SHG, dielectric relaxation, and spectroscopic techniques, information concerning the effect of hydrogen bonding on the chromophore orientational dynamics and intermolecular coupling can thus be examined.

The effect of hydrogen bonding on the temporal stability of chromophore orientation was also observed in the high molecular weight PP−PEPO ($\bar{M}_n$ ≈ 41 000 g/mol) matrix. Four temperatures, T_g − 140 °C, T_g − 90 °C, T_g − 20 °C, and T_g + 5 °C, were examined. As the final temperature decreases, the local free volume in the matrix decreases and prevents the chromophores from rotating out of the field-induced orientation, increasing the temporal stability of chromophore orientation following poling (Figure 11). This result is also consistent with those observed in the doped PMMA, poly(ethyl methacrylate), PIBMA, and polystyrene systems.[24,28,30] The differences in the activation energies required for chromophore orientation in the DO3- and DANS-doped systems were calculated. The Arrhenius equation, $y = \exp(-E_A/RT)$, was used to calculate the activation energy, E_A, as a function of temperature, T. y is the normalized $\chi^{(2)}(t)_{film}/\chi^{(2)}(t)_{MNA}$ at time t after the applied voltage was turned off. The normalized $\chi^{(2)}$ values at 6 and 12 min after the voltage was turned off at the final temperatures of T_g − 90 °C, T_g − 20 °C were taken as the y values. The difference in the activation energies calculated for the DO3- and DANS-doped systems was assumed to be due to hydrogen bonding. The two final temperatures were chosen for the calculations because there are less surface voltage persistence effects from corona poling at higher temperatures (i.e., charges tend to be trapped in the matrix at lower temperatures),[15b,c] thus the activation energy for hydrogen bonding calculated should be more reliable. It must be emphasized that these calculations were simple

(29) Silverstein, R. M.; Bassler, G. C.; Morrill, T. C. Infrared Spectrometry. In *Spectrometric Identification of Organic Compounds*, 5th ed.; John Wiley and Sons, Inc.: New York, 1991; pp 91−164.

(30) Dhinojwala, A.; Wong, G. K.; Torkelson, J. M. *J. Chem. Phys.* **1994**, *100*, 6046.

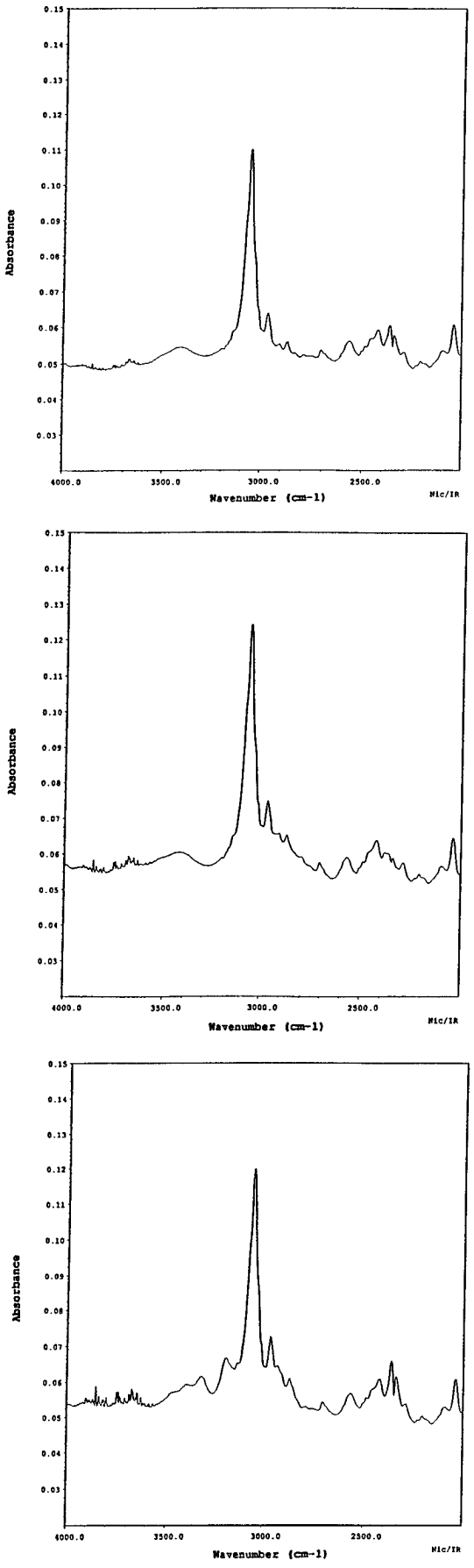

Figure 10. FTIR spectra for (a, top) undoped F_6 Bis A−PEPO, (b, middle) 10 wt % DANS-doped F_6 Bis A−PEPO, and (c, bottom) 10 wt % DO3-doped F_6 A−PEPO.

approximations in which the temperature dependence of activation energy was assumed to be of an Arrhenius

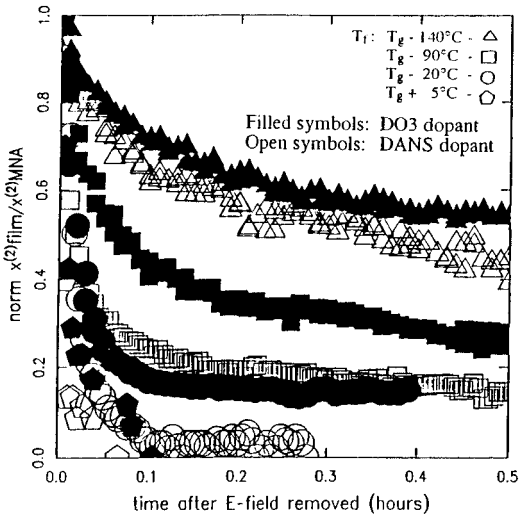

Figure 11. Effects of final temperature and hydrogen bonding on the temporal stability of chromophore orientation in 10 wt % DO3-doped and 10 wt % DANS-doped PP−PEPO ($\bar{M}_n \approx$ 41 000 g/mol) systems poled at −3500 V, T_g + 5 °C.

form, and the surface voltage effects were not taken into account. The activation energy for hydrogen bonding in this matrix was calculated to be around 3.7 kcal/mol. This value, as a first approximation, agrees with the literature (where typical hydrogen bonding energies of 3−10 kcal/mol were reported)[31] fairly well.

Effect of Chromophore Functionalization. The effect of chromophore functionalization on the relaxation behavior and intermolecular coupling was also investigated using dielectric relaxation. There are several advantages of derivatizing instead of doping the chromophores into the polymer matrices. Higher chromophore concentration can be incorporated without running into the problems of phase separation and/or dopant aggregation when the chromophores are covalently bonded to the polymer backbone. The T_g's are increased due to the enhanced rigidity of the polymer backbone and/or increased interchain cohesive forces.[4] Decomposition of chromophores is not a problem because they are part of the polymer chains. Furthermore, a better temporal stability of chromophore orientation may be achieved because of the stronger coupling between the covalently bonded chromophores and polymer backbone.[22,32]

Figure 12 shows the dielectric loss curves of PP−PEPO, PP−PEPO−pNPH, and PP−PEPO−DNPH. They were broader on the low-frequency side for the two-chain functionalized PP−PEPO systems than the undoped PP−PEPO, indicating stronger intermolecular coupling between the covalently bonded chromophores and polymer. It is noteworthy that PP−PEPO−DNPH exhibited a narrower loss curve than that of PP−PEPO−pNPH though the former polymer has an extra NO_2 group per repeat unit. This phenomenon contradicted to the observations reported in the literature and may be due to the defects that the extra NO_2 group

(31) (a) Joesten, M. D.; Schaad, L. J. *Hydrogen Bonding*; Marcel Dekker, Inc.: New York, 1974. (b) McMurry, J. *Organic Chemistry*, 2nd ed.; Brooks/Cole Publishing Co.: CA, 1988.

(32) (a) Huijts, R. A.; Jenneskens, L. W.; van der Vorst, C. P. J. M.; Wreesmann, C. T. J. *SPIE: Nonlinear Opt. Mater. II* **1989**, *1127*, 165. (b) Eich, M.; Sen, A.; Looser, H.; Bjorklund, G. C.; Swalen, J. D.; Twieg, R.; Yoon, D. Y. *J. Appl. Phys.* **1989**, *66*, 2559. (c) Kohler, W.; Robello, D. R.; Willand, C. S.; Williams, D. J. *Macromolecules* **1991**, *24*, 4589. (d) Shi, Y.; Ranon, P. M.; Steier, W. H.; Xu, C.; Wu, B.; Dalton, L. R. *Appl. Phys. Lett.* **1993**, *63*, 2168.

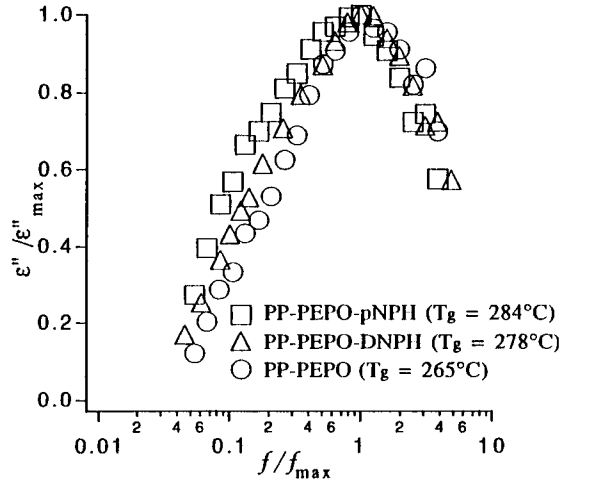

Figure 12. $\epsilon''/\epsilon''_{max}$ vs f/f_{max} for PP−PEPO, PP−PEPO−pNPH, and PP−PEPO−DNPH measured at $T_g + 15$ °C.

created in the PP−PEPO−DNPH matrix, resulting in a lower T_g (as determined by DSC) and weaker intermolecular cooperativity (as reflected by a narrower loss curve) than PP−PEPO−pNPH. The results of the Havriliak−Negami equation fits are shown in Table 3. The values of α increased in the order PP−PEPO−pNPH < PP−PEPO−DNPH < PP−PEPO, indicating that PP−PEPO−pNPH had the strongest intermolecular coupling. The lower certainty in the product $\alpha\beta$ is caused by the greater noise in the determination of β because of limitations of the frequency range of our equipment. The uncertainty in the symmetry is caused by the incomplete determination of the data for the full-frequency range at a given temperature because of the properties of the polymer itself. The SHG measurements on these two side-chain-functionalized systems will be performed, and the results will be correlated with those obtained using dielectric relaxation and published in the near future.[33]

Conclusions

Systematic studies on the effects of structure/property relationships on chromophore orientational dynamics and polymer relaxations in the thermally stable NLO polyarylene ethers have been performed. By combining SHG and dielectric relaxation, specific issues such as the effects of polymer backbone structures and molecular weight, chromophore/polymer interactions, and chromophore functionalization on the segmental relaxation behavior and intermolecular cooperativity in these polymer systems can be investigated. Attempts to correlate the molecular level parameters including the molecular weight and polydispersities to the observed physical properties were made. Although the temporal stability of dopant orientation observed in these polymer systems was not great compared with many thermally stable polymers reported in the literature,[3] the information obtained here is critical for better tailoring materials for optical device and engineering applications.

Changes in the polymer backbone structure affected the intermolecular cooperativity and segmental relaxations. The dielectric loss curve became broader, particularly on the low-frequency side, as the pendant groups on the polymer backbone became more polar and/or more sterically hindered, indicating that the segmental relaxations were more intermolecularly coupled. Second harmonic generation experiments also showed that chromophore disorientation following poling was retarded as the polymer chain segments became more intermolecularly coupled. The Havriliak−Negami equation and the Schonhals and Schlosser model were employed to fit and describe the dispersion curves. This was the first attempt, as far as we know, to employ this model to describe the extent of intermolecular interactions arising from various steric interferences, and as shown here the model can successfully correlate the values of α to the intermolecular coupling of the polymers.

For the specific polymer systems examined here, PP−PEPO with $\bar{M}_n$ of 41 000 and 16 000 g/mol, the loss curves were very similar. This indicates that the polymers had similar distribution of relaxation times and the intermolecular cooperativity remained minimally affected in the molecular weight range examined. Second harmonic generation experiments, however, showed that the 10 wt % DANS-doped PP−PEPO system with $\bar{M}_n$ of 41 000 g/mol had better short-term temporal stability at $T_g - 140$ °C following poling than the sample with $\bar{M}_n$ of 16 000 g/mol. This may be caused by the fact that there was less chain-end density in the high molecular weight sample, creating less free volume for the chromophores that were in the vicinity of the chain ends to rotate out of the poling-induced orientation. Since SHG is sensitive to changes in local microenvironment, a better short-term stability was observed in the high-molecular-weight system. However, the overall chromophore orientational dynamics was coupled to the polymer backbone motions. Because both systems were above the entangled level and had similar intermolecular coupling, the overall stability remained similar.

The effect of hydrogen bonding on the chromophore orientational dynamics and intermolecular coupling was investigated by combining SHG, dielectric relaxation, and spectroscopic techniques. Greater intermolecular cooperativity and better temporal stability of chromophore orientation following poling in the DO3-doped compared to the DANS-doped polymer systems with $\bar{M}_n$ of 15 000 and 41 000 g/mol were observed because of the hydrogen-bonding effect. Finally, the dispersion curves were broader, particularly on the low-frequency side, for the two side-chain functionalized systems, PP−PEPO−pNPH and PP−PEPO−DNPH, than the undoped PP−PEPO, indicating stronger intermolecular coupling between the covalently bonded chromophores and polymer.

Acknowledgment. We gratefully acknowledge the Office of Naval Research, the Department of Education, and Society of Photo-Optical Instrumentation Engineers (CYSF) for supporting this work. We wish to thank Mr. Daniel Riley (Department of Chemistry, VPI) for helpful discussions regarding the characterization of the polymers investigated.

CM9504100

(33) Fu, C. Y. S.; Lackritz, H. S.; Priddy, Jr., D. B.; McGrath, J. E., manuscript in preparation.
(34) Bondi, A. *J. Phys. Chem.* **1964**, *68*, 441.